and theoretical spectra deteriorates rather fast for increasing neutron angles. This is to be expected since the relative importance of the nonresonant amplitude, i.e., the amplitude corresponding to the simultaneous breakup in three nucleons, is increasing with respect to the amplitude representing the sequential decay, resulting in a proton-proton pair with low relative energy. The present calculation does not give the absolute value of the differential cross section. A normalization factor was obtained by matching the experimental and theoretical peaks in the 5° spectrum. It should be noticed that the angular dependence of the experimental spectra is reasonably accounted for in the calculated spectra.

From the present experiment we can conclude that the shape of the forward-angle neutron spectra is fairly well given by the above-described formalism using for the proton-proton interaction a scattering length of -7.778 F and an effective range of 2.714 F.

The discrepancy indicated in Fig. 16 between the present results and the calculation of Castillejo and Singh[29] is probably due to the limited validity of the impulse approximation at such a low energy.

ACKNOWLEDGMENTS

The authors are very much indebted to Martin Smith, who prepared the computer program for the calculation of the spectrometer resolution and efficiency. We also express our thanks to S. Plunkett and the cyclotron staff for their valuable assistance.

PHYSICAL REVIEW VOLUME 171, NUMBER 4 20 JULY 1968

$E2$ and $M1$ Matrix Elements in B^{10}†

E. K. WARBURTON, J. W. OLNESS, S. D. BLOOM,* AND A. R. POLETTI‡
Brookhaven National Laboratory, Upton, New York
(Received 26 January 1968)

γ-ray decay of the B^{10} 2.15- and 3.59-MeV levels was studied following population via the $B^{11}(He^3,\alpha)B^{10}$ reaction at $E_{He^3}=2.6$ MeV. The γ rays were detected in coincidence with α particles observed in an axially symmetric silicon detector centered at 180° to the beam. γ-ray branching ratios were extracted for both levels. From the angular distributions of the decay γ rays, results were obtained for the $E2/M1$ mixing ratios x of the decay of the 2^+ 3.59-MeV level to the 3^+ ground state, the 1^+ 0.72-MeV level, and the 1^+ 2.15-MeV level, respectively, as follows: $+0.31<x<+2.1$, $x^{-1}=+(0.11\pm0.10)$, $x=-(0.38\pm0.09)$, all pertaining to $\Delta T=0$ transitions. For the decay of the 2.15-MeV level to the 0.72-MeV level, $x=-(0.29\pm0.05)$ or $-(3.39\pm0.55)$. Combining these results with previous work gives information on the magnitudes as well as the relative phases of the $M1$ and $E2$ matrix elements considered. These results are compared with the predictions of the independent-particle model.

I. INTRODUCTION

THE nucleus B^{10} lying midway along the $1p$ shell and with $N=Z$ has a "complicated" spectrum of low-lying levels and represents an interesting and exacting challenge to our understanding of nuclear structure. The level scheme of those states belonging to the s^4p^6 configuration is reproduced quite well by the independent-particle model (IPM),[1–3] but IPM calculations[3,4] do not appear to give a completely satisfactory account of the total radiative widths of these levels.[5,6]

The known transitions connecting the bound s^4p^6 states of B^{10} are all either $M1$ or $E2$, or a mixture of both. Comparisons between experiment and the IPM have been hampered by a lack of knowledge concerning the relative intensities of the $M1$ and $E2$ contributions in those transitions that are mixed. Since the total radiative widths and branching ratios for the bound states of B^{10} are known, a determination of the $E2/M1$ mixing ratios for the mixed transitions would subsequently determine the partial $M1$ and $E2$ widths, which could then be compared separately to the IPM predictions.

Further information of considerable importance would be provided by these results, namely, the relative phases of the $E2$ and $M1$ matrix elements.[7] That the signs of

† Work performed under the auspices of the U. S. Atomic Energy Commission.
* Summer visitor during 1967. Permanent address: Lawrence Radiation Laboratory, Livermore, Calif.
‡ Now at Lockheed Palo Alto Research Laboratory, Palo Alto, Calif.
[1] D. R. Inglis, Rev. Mod. Phys. **25**, 390 (1953).
[2] D. Kurath, Phys. Rev. **101**, 216 (1956).
[3] S. Cohen and D. Kurath, Nucl. Phys. **73**, 1 (1965); D. Kurath, Argonne National Laboratory Report No. ANL-7108, 1965 (unpublished).
[4] D. Kurath, Phys. Rev. **106**, 975 (1957).
[5] D. E. Alburger, P. D. Parker, D. J. Bredin, D. H. Wilkinson, P. F. Donovan, A. Gallmann, R. E. Pixley, L. F. Chase, Jr., and R. E. McDonald, Phys. Rev. **143**, 692 (1966).
[6] E. K. Warburton, J. W. Olness, K. W. Jones, C. Chasman, R. A. Ristinen, and D. H. Wilkinson, Phys. Rev. **148**, 1072 (1966).
[7] H. J. Rose and D. M. Brink, Rev. Mod. Phys. **39**, 306 (1967); A. R. Poletti, E. K. Warburton, and D. Kurath, Phys. Rev. **155**, 1096 (1967).

these mixing ratios be correctly predicted by the model is admittedly a less stringent criterion of its success than that the calculations reproduce the magnitudes of the $M1$ and $E2$ matrix elements. It is nevertheless a necessary criterion and ought therefore to be applied in gauging the success of the model. For even if the IPM succeeds in correctly reproducing the magnitudes of the $M1$ and $E2$ matrix elements, it is possible that such agreement is only fortuitous, in that the relative phases may be incorrect. For cases where the model has done poorly in predicting the magnitudes of these matrix elements an examination of the relative phases becomes quite interesting indeed.

Our specific intent in the present investigation was to obtain information on the $E2/M1$ amplitude ratios for the mixed transitions connecting the bound states of B^{10}, through angular-distribution studies of the decay γ rays relative to the beam direction following formation of the B^{10} initial state by the $B^{11}(He^3,\alpha)B^{10}$ reaction. The γ-decay modes of the bound levels of B^{10} are illustrated in Fig. 1, which shows the energy-level scheme of B^{10} as determined by this and earlier work. The initial states whose decays we investigated are those at 2.15 and 3.59 MeV. γ rays from the decay of these levels were observed in coincidence with the reaction α particles that were detected in an axially symmetric counter centered at 180° to the beam. The population parameters describing the alignment of the initial state were subsequently obtained from the γ-ray angular distributions simultaneously with the $E2/M1$ amplitude ratios of the mixed transitions. The experimental problem presented here and the method of approach used are quite similar to that involved in several previous studies at this laboratory.[8,9]

We note that, for the $B^{11}(He^3,\alpha\gamma)B^{10}$ reaction, the detection of the α particles at $\theta_\alpha \sim 180°$ does not *a priori* limit the magnetic substates in which the B^{10} initial state may be found; but it *does*, in fact, determine the population of these substates and thereby the alignment. For comparison, an experimental measurement of the angular distribution of the same γ-rays observed in singles (α particles unobserved) revealed that the alignment achieved in this case was much weaker than with the α-particle coincidence condition. The coincidence condition also led to a convenient sorting of the γ rays into groups associated with each B^{10} level, which considerably aided the distribution analysis.

II. EXPERIMENTAL PROCEDURE AND RESULTS

A. General Procedure

Angular correlations in the $B^{11}(He^3,\alpha\gamma)B^{10}$ reaction were measured at a bombarding energy $E_{He^3}=2.60$ MeV, employing for this purpose a scattering chamber that has been described previously.[10,11] The target for these measurements was composed of a double thickness of 50-μg/cm^2 foil of enriched B^{11}, thus providing a 100-μg/cm^2 target representing a thickness of about 60 keV to the He^3 beam. The foils were affixed to a brass-ring holder placed at the center of the scattering chamber, with the normal to the target face set at 30° to the beam direction. γ rays were detected in a 5-in.-diam by 6-in.-long NaI(Tl) detector, located with its front face at a distance 18.5 cm from the target and set at one of 6 discrete angles in the range $0° \leqslant \theta_\gamma \leqslant 90°$. Within this angular range the walls of the brass scattering chamber were only 0.015 in. thick; the beam-stop assembly was also made of lightweight material in order to minimize absorption in the region $\theta_\gamma \sim 0°$.

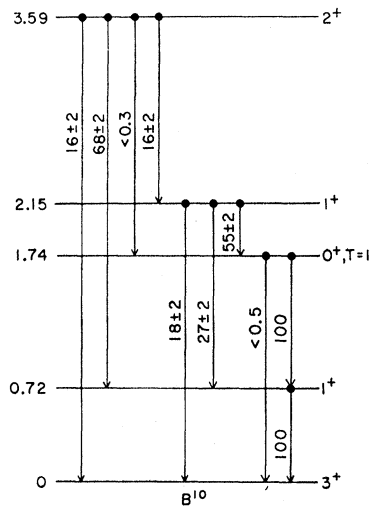

FIG. 1. Level scheme of the bound states of B^{10}. The γ-ray branching ratios (in %) are an average of the present work with the values summarized in Ref. 6.

Charged particles emanating from the target were detected in an annular surface-barrier detector centered at 180° to the He^3 beam and at a distance of 2.2 cm from the target. A circular collimator shielded the front face of the detector and also restricted its view to particles emerging in the range $\theta_\alpha = 162 \pm 8°$. The detector itself was an 890-Ω cm ORTEC device of 300-mm^2 area with a central aperture of 4 mm diam, operated at a bias voltage of 50 V producing a depletion depth of 105 μ. This was sufficient to stop all α groups of interest from the $B^{11}(He^3,\alpha)B^{10}$ reaction, while protons would produce, at most, pulses corresponding to 3.3 MeV.

Time-coincident pulses from the particle and γ-ray detectors were analyzed by a TMC 2^{14}-channel analyzer operated in a $512(\gamma)\times 32(\alpha)$-channel mode. Coincidence requirements were imposed by an external fast-

[8] E. K. Warburton, J. W. Olness, D. E. Alburger, D. J. Bredin, and L. F. Chase, Jr., Phys. Rev. **134**, B338 (1964).
[9] A. R. Poletti, J. W. Olness, and E. K. Warburton, Phys. Rev. **151**, 812 (1966).
[10] J. W. Olness and E. K. Warburton, Phys. Rev. **151**, 792 (1966).
[11] E. K. Warburton, J. W. Olness, and A. R. Poletti, Phys. Rev. **160**, 938 (1967).

slow coincidence circuit ($2\tau \sim 80$ nsec), which provided the analyzer gating signal. The angular-correlation measurements consisted of two sets of coincidence data recorded, in random order, at each of the six γ-detector angles $\theta_\gamma = 0°$, 20°, 30°, 45°, 60°, and 90°. The results of each run were stored on magnetic tape for later computer analysis as has been described previously.[10] At the conclusion of these measurements the 12 sets of data were added together to form a summed spectrum that was analyzed to determine branching ratios and line shapes.

Pertinent results from an analysis of the "summed spectrum" are shown in Fig. 2. The main plots show the γ spectra measured in coincidence with α groups 2, 3, and 4 populating, respectively, the 1.74-, 2.15-, and 3.59-MeV levels of B^{10}. The various γ-ray photopeaks are identified according to transition energy, and also by the energies of the initial and final states of B^{10} between which the transitions occur. The corresponding α spectrum measured in coincidence with γ rays of energy >0.8 MeV is shown in the inset. (We note that although the experimental resolution was not sufficient to resolve the 1.74- and 2.15-MeV α groups, the 2-parameter analysis permitted a *complete* separation of the γ spectra coincident with these two α groups.) These data were acquired with a beam current of 50 nA, which was within a factor of ~ 2 of the maximum the target could withstand without damage. At this relatively low current, the ratio of reals/randoms was about 20/1.

At each angle 2-parameter data were acquired for $\sim 5\frac{1}{2}$ hours for a net charge deposited of $\sim 930\ \mu$C. Thus the spectrum shown in Fig. 2 represents about 3 days of continuous running for a net bombardment of 0.011 C. The solid-state particle detector exhibited no observable gain drift over this period; the γ-detector gain was stabilized by a Cosmic Radiation Laboratories "Spectrastat" set on the 0.511-MeV annihilation peak, which appeared strongly in the γ singles spectrum. All of the γ-ray peaks shown in Fig. 2 are somewhat broadened by Doppler effects because these data are the sum of the

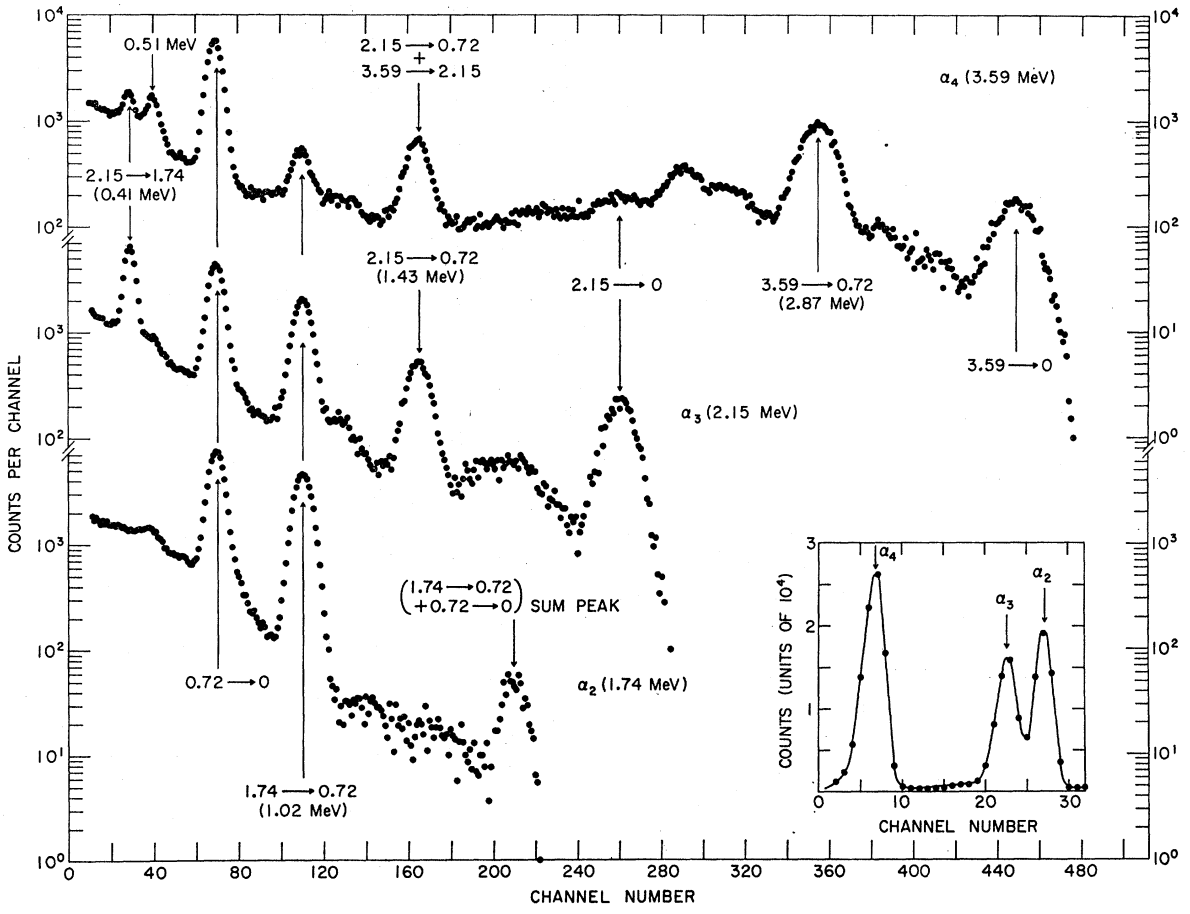

FIG. 2. Spectra of γ rays from the $B^{11}(He^3,\alpha)B^{10}$ reaction measured in coincidence with α-particle groups α_2, α_3, and α_4 populating, respectively, the 1.74-, 2.15-, and 3.59-MeV levels of B^{10}. For each spectrum, the γ-ray peaks are labeled by the energies (in MeV) of the initial and final states between which the transitions occur and, in most cases, by the energy of the γ ray. These spectra were obtained from the sum of all the two-parameter data for $E_{He^3} = 2.60$ MeV. The insert shows the α-particle spectra in coincidence with all γ-ray pulses with energies greater than 800 keV.

data taken at 6 different angles. Because the B^{10} nuclei recoiled into vacuum *all* γ rays had the full Doppler shift allowed by the kinematics ($\sim$3% between the 0° and 90° spectra) irrespective of the lifetime of the initial level; these shifts were readily observed in the individual correlation data.

B. γ-Ray Branching Ratios

For each of the γ rays evident in Fig. 2 the area of the photopeak was determined by spectrum stripping. These areas were then corrected for the differential absorption in the target chamber walls (amounting to a maximum of $\sim$4% for the 0.41-MeV line) and also for the effects of summing of various cascade transitions which would augment the measured intensity of the crossover transitions. These data were also corrected for correlation effects using the results given in the next subsection. Since the "summed spectrum" is essentially an average over the six angles of the correlation measurement, these latter corrections were small ($\lesssim$10%). Finally, the relative intensities and branching ratios were computed, using photopeak efficiency curves appropriate to a 5×6-in. NaI(Tl) detector at 18.5-cm source-crystal distance.

In the results shown in Fig. 2 for the γ spectrum measured in coincidence with group α_2 (1.74-MeV level) we see intense γ rays of energy 0.72 and 1.02 MeV, from the $1.74 \rightarrow 0.72 \rightarrow 0$ cascade transition. The peak at 1.74 MeV ($\sim$1% intensity) matches within experimental error the intensity computed for summing of 1.02- and 0.72-MeV γ rays, and we are subsequently able to set an upper limit of $<0.5\%$ on a possible $1.74 \rightarrow 0$ ground-state decay.

The middle plot of Fig. 2 shows the γ rays coincident with group α_3 (2.15-MeV level). The weak peak at 0.51 MeV in this spectrum [and also in that for group α_4 (3.59-MeV level)] arises primarily from real coincidences between α particles and annihilation radiation produced in the target chamber walls (brass) by the higher-energy γ rays ($E_\gamma > 1.02$ MeV) from this B^{10} level. After appropriate corrections for summing and also for absorption and correlation effects, we arrive at the following branching ratios for the decay of the 2.15-MeV level to the indicated final states: 0.0 MeV (17.5%), 0.72 MeV (26.3%), and 1.74 MeV (56.2%), all with an uncertainty of $\pm$2%. These are in excellent agreement with the respective weighted averages of previous measurements[6]: 22±8%, 26±2%, and 52 ±4%, and we now adopt for these transitions the branching ratios shown in Fig. 1.

From the data shown in Fig. 2 for the γ rays coincident with group α_4 (3.59-MeV level) we deduce the following branching ratios for de-excitation of the 3.59-MeV level to the indicated final levels: 0.0 MeV (16.6%), 0.72 MeV (68.1%), and 2.15 MeV (15.4%), all with an uncertainty of $\pm$2%. Again, this is in excellent agreement with the weighted average of previous measurements[6]: 15±2%, 67±2%, and 18±3%, respectively. An upper limit of $<0.3\%$ has previously been placed[12] on a possible $3.59 \rightarrow 1.74$ transition; this is appreciably more restrictive than the limit $<5\%$ which can be derived from the present experiment. We adopt as best values the branching ratios shown in Fig. 1.

As a final consideration, the various data of Fig. 2 were used to check the curve of absolute photopeak efficiency ϵ_p versus γ-ray energy E_γ. This was possible since in several cases the branching-ratio information is overdetermined; i.e., for the decay of the 1.74-MeV level $I_\gamma(1.02) = I_\gamma(0.72)$, and for the 2.15-MeV level, $I_\gamma(0.72) = I_\gamma(1.02) + I_\gamma(1.43)$; $I_\gamma(0.41) = I_\gamma(1.02)$, etc. These checks were found to be consistent to within $\sim$5%, which is roughly the relative error we assign to our ϵ_p versus E_γ curve over the range 0.4–3.6 MeV. The curve of ϵ_p versus E_γ actually used in all of these computations was generated for a 5×6-in. NaI(Tl) detector by extrapolation procedures based on the extensive information available on 3×3-in. NaI(Tl) detectors,[13] 5×5-in. NaI(Tl) detectors,[14,15] and also on some results for 4×4-in. NaI(Tl) detectors.[16] The γ-ray total absorption calculations of Rutledge[17] for a 5×6-in. NaI(Tl) crystal were also useful. The resultant extrapolated curve for a 5×6-in. NaI(Tl) detector at 18.5 cm is, of course, very similar to that for a 5×5-in. NaI(Tl) detector, but is increased by a small constant factor and has a somewhat more gradual slope.

C. γ-Ray Angular Correlations

The angular-correlation information was extracted in a straightforward way by determining the net area of the various α-γ coincidence peaks evident in the individual 2-parameter data.

Normalization factors for the various data were based on: (1) net charge deposited on the beam collector during the course of the measurement and (2) the number of α particles in the group α_4 (3.59-MeV level) as determined by a voltage gate and scaler set on this peak as seen in the particle detector. The over-all agreement between the factors based on (1) and (2) was excellent (within 1.5%) and thus an average factor was adopted for each measurement. The axial alignment of the (rotating) 5×6-in. NaI(Tl) detector was determined geometrically[10] to about 1.5%. The γ-absorption effects due to the thin chamber walls and beam-stop assembly were known to comparable accuracy. Thus the net error

[12] R. E. Segel, P. P. Singh, S. S. Hanna, and M. A. Grace, Phys. Rev. **145**, 736 (1966).
[13] R. L. Heath, Phillips Petroleum Co. Report No. IDO-16408, 1955 (unpublished).
[14] S. H. Vegors, L. L. Marsden, and R. L. Heath, Phillips Petroleum Co. Report No. IDO-16370, 1958 (unpublished).
[15] F. C. Young, H. T. Heaton, G. W. Phillips, P. D. Forsyth, and J. B. Marion, Nucl. Instr. Methods 44, 109 (1966).
[16] K. L. Coop and H. A. Grench, Lockheed Missiles and Space Corp. Report No. LMSC 6-75-65-37, 1965 (unpublished).
[17] A. R. Rutledge, Atomic Energy of Canada, Ltd. Report No. CRP-851, 1959 (unpublished).

introduced into the correlation measurements, due to both geometric uncertainties and normalization procedures, is estimated to be $\lesssim 2\%$. A check on geometrical and normalization uncertainties was provided by the angular distributions of those γ rays de-exciting the 0^+ 1.74-MeV level (see Figs. 1 and 2). These must be isotropic and were found to be so within the statistical errors of the measurement, which were $\sim 1.5\%$.

Least-squares Legendre-polynomial fits to the correlation data, of the form $W(\theta)=\sum_k A_k P_k(\theta)$, were obtained for the transitions of particular interest; the results are listed in Table I. The 3.59- and 2.15-MeV levels have $J^\pi=2^+$ and 1^+, respectively; thus for these states the maximum values of k are 4 and 2, respectively. The goodness-of-fit parameter χ^2 listed in Table I has been normalized to the degrees of freedom and therefore has an expectation value of unity if the internal (experimental) errors are both realistic *and* uncorrelated. If the internal errors are correlated (i.e., the error matrix is not diagonal) then the normalized χ^2 will have a value different from unity and, in fact, will be equal to the ratio of the internal to the external errors (for a correct solution).[18]

That the (normalized) values of χ^2 in Table I tend to be less than unity suggests that the internal errors, representing individually the sum of the statistical errors and the estimated systematic errors for each data point, are correlated, so that the corresponding external errors are reduced. Since the estimated systematic errors are essentially those of the spectrum stripping process it is not surprising that such correlations should appear, since there is very likely a correlation between the stripping errors at the various angles.

The angular distribution of the 2.15-MeV γ ray measured in coincidence with group α_3 was also determined. Although consistent with expectations, this distribution provided no information that was useful in determining the $E2/M1$ amplitude ratios of the mixed transition originating from the 2.15-MeV state. The main reason for this is that a $1^+ \rightarrow 3^+$ quadrupole transition has an angular distribution that is inherently not far from isotropy. For this case the possible variation of its A_2 coefficient with the degree of alignment was comparable to the experimental uncertainty in the determination of this coefficient and thus the measured distribution places no restriction on the population parameters. For the same reason, the angular distributions of 0.72-MeV γ rays measured in coincidence with groups α_3 and α_4 were of no use in determining the mixing ratio of those mixed transitions leading to the 0.72-MeV state. In addition, the 0.72-MeV level is long lived enough, $\tau=1$ nsec,[19] so that the angular correlation of the $0.72 \rightarrow 0$ transition is attenuated by partial loss of alignment before γ emission.

TABLE I. Results of an even-order Legendre-polynomial fit to various correlation data from $B^{11}(He^3,\alpha)B^{10}$. The coefficients have been corrected for the finite size of the γ-ray detector.

Transition (MeV)	A_2/A_0	A_4/A_0	χ^2
$2.15 \rightarrow 1.74$	$+(0.30\pm0.01)$	...	1.00
$2.15 \rightarrow 0.72$	$-(0.39\pm0.02)$	...	0.99
$3.59 \rightarrow 2.15$	$+(0.18\pm0.04)$	$+(0.10\pm0.06)$	0.56
$3.59 \rightarrow 0.72$	$+(0.04\pm0.04)$	$+(0.53\pm0.05)$	0.86
$3.59 \rightarrow 0$	$+(0.21\pm0.03)$	$+(0.08\pm0.04)$	0.39
$3.59 \rightarrow 2.15 \rightarrow 1.74$	$-(0.30\pm0.06)$	...	0.30

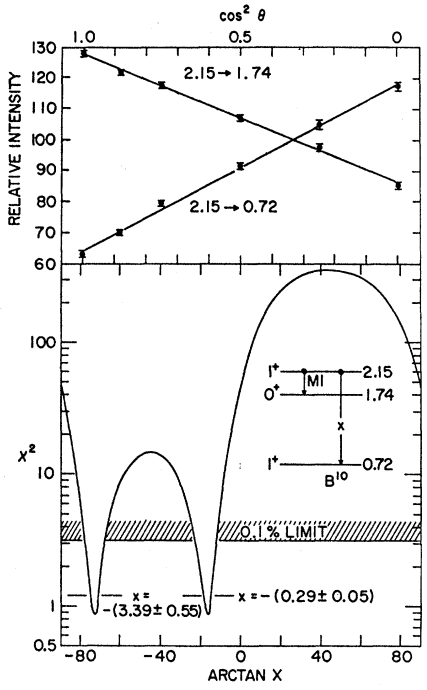

FIG. 3. α-γ angular correlation results for the B^{10} $2.15 \rightarrow 0.72$ and $2.15 \rightarrow 1.74$ transitions following population of the 2.15-MeV level in the $B^{11}(He^3,\alpha)B^{10}$ reaction. The points with error bars (upper plot) show the experimental correlation data. The results of a simultaneous χ^2 analysis of the data for both transitions are shown in the lower figure. Here we have plotted χ^2, representing goodness-of-fit to the experimental data, as a function of arctan$x$, where x is the $E2/M1$ mixing ratio in the $2.15 \rightarrow 0.72$ transition. The probability that χ^2 exceeds the limit marked as 0.1% is just 0.1%. It is seen that there are two possible solutions for x. These values and their standard deviations are indicated. The solid curves in the upper plot are the best fits for $x=-0.29$ or -3.39.

III. ANALYSIS OF THE ANGULAR CORRELATIONS

A. 2.15-MeV Level

The analysis of these γ-ray angular-correlation results follows procedures that have been well described previ-

[18] A. J. Ferguson, *Angular Correlation Methods in Gamma-Ray Spectroscopy* (North-Holland Publishing Co., Amsterdam, 1965).
[19] F. Ajzenberg-Selove and T. Lauritsen, Nucl. Phys. **78**, 1 (1966).
[20] A. R. Poletti and E. K. Warburton, Phys. Rev. **137**, B595 (1965).

ously.[8,9,20] The results obtained for the decay of the 2.15-MeV level, illustrated in Fig. 3, exemplify the method. We are interested in the $E2/M1$ mixing ratio of the $2.15 \rightarrow 0.72$ transition (see Fig. 1). Simultaneous least-squares fits were made to the angular correlation data for the $2.15 \rightarrow 1.74$ (pure $M1$) and $2.15 \rightarrow 0.72$ transitions for discrete values of the mixing ratio of the latter. The relative probabilities $P(0)$ and $P(1)$, for populating the $m=0$ and ± 1 substates of the 2.15-MeV level were the variables in this fit. For each value of the mixing ratio x, best values for $P(0)$ and $P(1)$ were obtained as well as a value for χ^2. The lower curve of Fig. 3 shows $\arctan x$ versus χ^2. There are two acceptable solutions for x. For a $1 \rightarrow 1$ $E2/M1$ transition the two solutions for x happen to be reciprocals of one another. The solid curves in the upper part of Fig. 3 are the best fits to the correlation data for these two solutions, which give the identical results $P(0)=0.130\pm0.003$, $P(1)=0.435\pm0.002$, with $P(1)=P(-1)$ and $P(0)+2P(1)=1$. To a confidence of 99.9% (the 0.1% limit of Fig. 3) x lies in one of the two regions $-0.42<x<-0.12$ or $-4.7<x<-2.3$. The best values of x are $-(0.29\pm0.05)$ or $-(3.4\pm0.55)$, where the uncertainties correspond to one standard deviation. The phase convention used throughout this paper for $E2/M1$ mixtures is that of Ref. 7.

Essentially the same analysis of correlation data for the B^{10} $2.15 \rightarrow 0.72$ transition has been made twice previously. Lonergan and Donahue[21] found that this transition was essentially either pure $M1$ or $E2$, $|x|<0.1$ or >10, while MacDonald *et al.*[22] obtained the result $x=-(0.23_{-0.06}{}^{+0.05})$ or $-(4.1_{-1.0}{}^{+0.7})$. Our results are in strong disagreement with the former conclusion but in good agreement with the latter. We adopt the weighted average of our results and those of MacDonald *et al.*[22]:

$$x=-(0.267\pm0.040) \quad \text{or} \quad -(3.75\pm0.55).$$

In principle, the ambiguity in x could be removed by a simultaneous measurement of the angular distribution of the 0.72-MeV γ ray in the $2.15 \rightarrow 0.72 \rightarrow 0$ cascade. In practice, however, this distribution was not determined with sufficient accuracy to differentiate between the two possible values of x. The reasons for this were discussed at the end of Sec. II.

B. 3.59-MeV Level

In Fig. 4 are shown the results of least-squares fits to the $3.59 \rightarrow 0$ and $3.59 \rightarrow 0.72$ distribution data. These preliminary fits are shown to illustrate the fact that there is not enough information in the distribution for either transition to determine a "solution" for its $E2/M1$ mixing ratio. This is not surprising since there

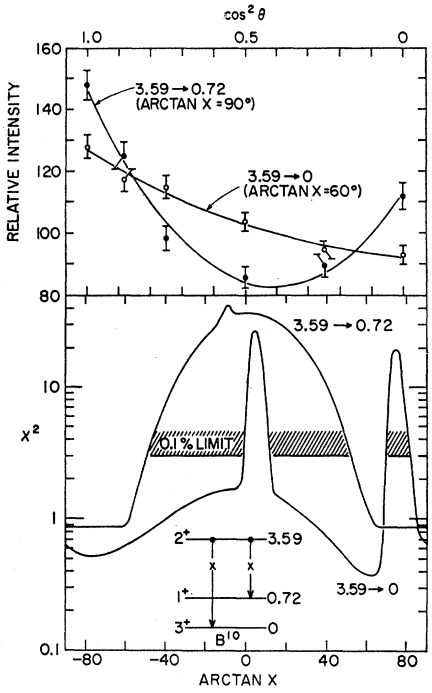

FIG. 4. α-γ angular correlation results for the B^{10} $3.59 \rightarrow 0$ and $3.59 \rightarrow 0.72$ transitions. The points with error bars (upper curve) show the experimental correlation data. The results of independent χ^2 analysis of these two correlations, treated separately, are shown in the lower plot. In both cases x is the $E2/M1$ mixing ratio of the transition. Best fits to the correlation data are given by the solid curves in the upper plot. These correspond to the indicated values of x. It is seen that the $3.59 \rightarrow 0.72$ transition must be predominantly $E2$ ($\arctan|x|>50°$) but that only small regions of x are excluded for the $3.59 \rightarrow 0$ transition.

are more unknowns (x and two parameters to define the alignment of the initial state) than measured variables (A_2 and A_4 coefficients) for a fit to a single distribution. Nevertheless some information on the mixing ratios is obtained because the equations are constrained, i.e., the $P(m)$'s are positive-definite and the dependence of the angular distributions on the $P(m)$'s and on x is specified. For example, the expression for A_2 for the $3.59 \rightarrow 0$ transition is proportional to a quadratic in x with two roots and for these two roots we have $A_2=0$, in disagreement with experiment (see Table I and the upper part of Fig. 4). Thus, the χ^2-versus-$\arctan x$ curve for this transition shows peaks at these roots. For the $3.59 \rightarrow 0.72$ transition the A_4 coefficient was quite large (see Table I) and since it is proportional to x^2 we obtain a lower limit on $|x|$, $|x|>1.2$ at the 0.1% limit, from the fit of Fig. 4.

A simultaneous fit to the angular distribution data for the two members of the cascade: $3.59 \rightarrow 2.15 \rightarrow 1.74$ is shown in Fig. 5. It is seen that for this fit there are two solutions for the mixing ratio of the $3.59 \rightarrow 2.15$ transition. If now, however, we include the $3.59 \rightarrow 0.72$ transition in this fit, with no restriction on its mixing ratio, we obtain the χ^2-versus-$\arctan x$ curve of Fig. 6.

[21] J. A. Lonergan and D. J. Donahue, Bull. Am. Phys. Soc. **11**, 27 (1966).
[22] J. R. MacDonald, D. F. H. Start, and D. H. Wilkinson (to be published).
[23] E. K. Warburton, D. E. Alburger, A. Gallmann, P. Wagner, and L. F. Chase, Jr., Phys. Rev. **133**, B42 (1964).

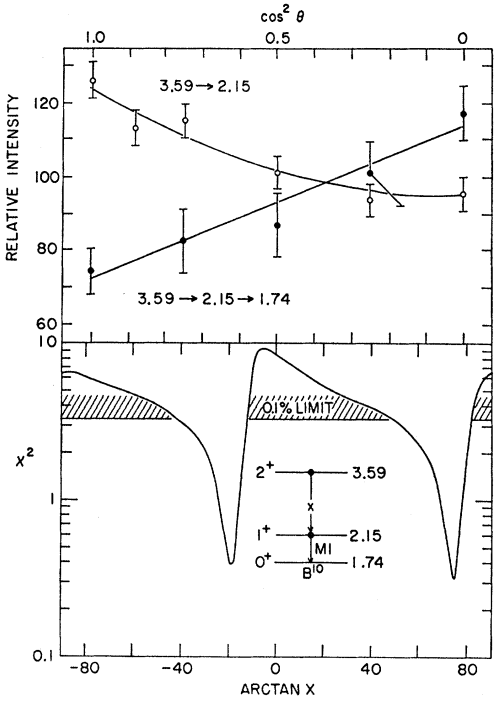

FIG. 5. α-γ correlation results for the B^{10} $3.59 \rightarrow 2.15 \rightarrow 1.74$ cascade. The points with error bars (upper plots) show the correlation data for the two members of the cascade. The results of a simultaneous χ^2 analysis of the data for the two members of the cascade are shown in the lower figure. It is seen that there are two possible solutions for x, the $E2/M1$ mixing ratio of the $3.59 \rightarrow 2.15$ transition. The solid curves in the upper plot are the best fits to the data for the solution near $\arctan x = -20°$.

(Exactly the same result would have been obtained if we had restricted x for the $3.59 \rightarrow 0.72$ transition to $|x| > 1.2$.) It is seen that only one solution for the mixing ratio of the $3.59 \rightarrow 2.15$ transition remains. The other solution corresponds to an alignment of the 3.59-MeV level which is not consistent with the angular distribution of the $3.59 \rightarrow 0.72$ transition.

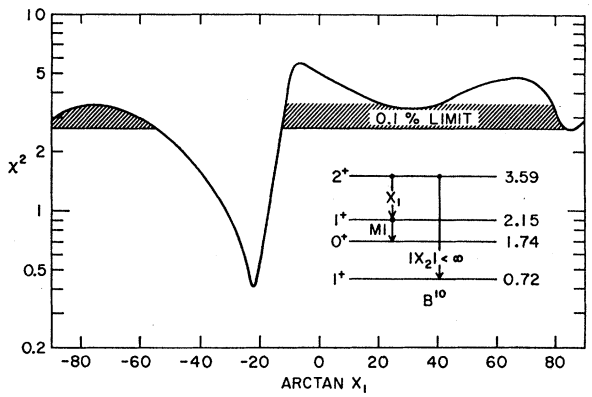

FIG. 6. α-γ angular correlation results for the B^{10} $3.59 \rightarrow 2.15$ transition. The χ^2 analysis was performed on the angular correlation data for the three transitions indicated in the insert. The mixing ratio of the $3.59 \rightarrow 0.72$ transition was freely varied as indicated and the envelope of the minimum value of χ^2 is shown as a function of $\arctan x_1$. This analysis eliminates the positive solution for the $E2/M1$ mixing ratio of the $3.59 \rightarrow 2.15$ transition which was allowed by the analysis illustrated in Fig. 5.

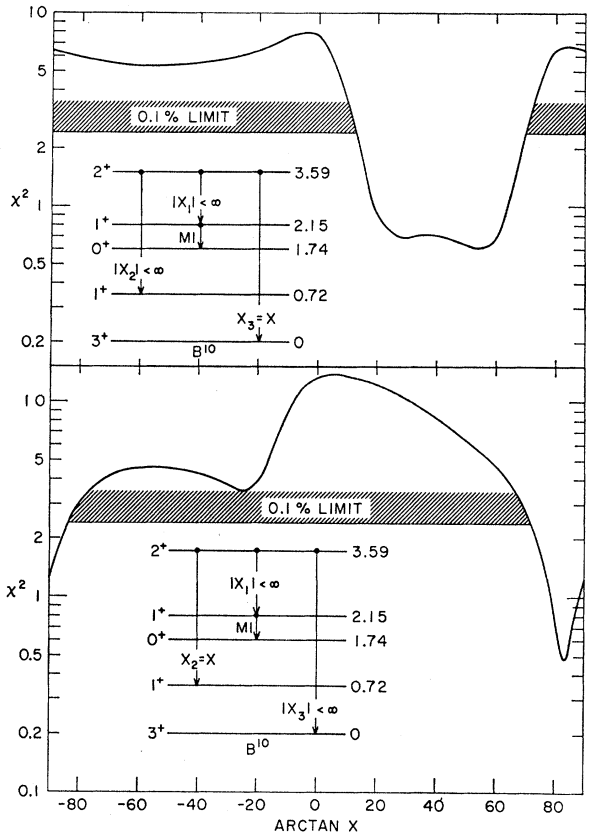

FIG. 7. α-γ angular correlation results for the B^{10} $3.59 \rightarrow 0$ transition (upper plot) and $3.59 \rightarrow 0.72$ transition (lower plot). The two χ^2 plots are from the same simultaneous analysis of the data for all four transitions indicated in the insert. In each plot 2 of the 3 mixing ratios shown in the inserts were freely varied and the envelope of the minimum value of χ^2 is shown as a function of the remaining mixing ratio. The restrictions on the mixing ratios of the $3.59 \rightarrow 0$ and $3.59 \rightarrow 0.72$ transitions quoted in the text were obtained from these plots.

TABLE II. Summary of experimental results for the γ decay of the B^{10} 2.15- and 3.59-MeV levels.

E_i (MeV)	E_f (MeV)	Branching ratios (%)	x $(E2/M1)$[a]	Γ_γ[b] (10^{-4} eV)
2.15	0.0	18±2	···	$0.49_{-0.07}^{+0.10}$
	0.72	27±2	$-(3.75\pm0.55)^{\pm1}$	$0.74_{-0.11}^{+0.15}$
	1.74	55±2	···	$1.51_{-0.21}^{+0.30}$
				$\Gamma_\gamma(\text{tot.}) = 2.74_{-0.40}^{+0.55}$
3.59	0.0	16±2	$+(1.5\ \pm0.6)$	$6.8_{-0.60}^{+0.74}$
	0.72	68±2	$+(0.11\pm0.10)^{-1}$	$28.9_{-2.5}^{+3.1}$
	1.74	<0.3	···	<0.15
	2.15	16±2	$-(0.38\pm0.09)$	$6.8_{-0.60}^{+0.74}$
				$\Gamma_\gamma(\text{tot.}) = 42.5_{-3.7}^{+4.6}$

[a] The phase convention is that of Ref. 7.
[b] Based on the Γ_γ(tot.), which are from Ref. 25, and the branching ratios given in the third column.

TABLE III. Comparison between experiment and IPM predictions for the $M1$ and $E2$ radiative widths connecting the s^4p^6 states of B^{10}. The columns labeled $a/K=4.5$ are from Ref. 4 while the other IPM predictions are from Ref. 3. The $\Delta T=0$ $E2$ widths contain a collective enhancement $(1+\beta_p+\beta_n)^2$ of 4.0 while the $\Delta T=1$ $E2$ width has no collective enhancement. A radial integral $\langle r^2\rangle_{1p1p}$ of 7.056 F^2 was used for the $E2$ widths.

			$\Gamma_\gamma(M1)$ (10^{-4} eV)					$\Gamma_\gamma(E2)$ (10^{-4} eV)				
E_i (MeV)	E_f (MeV)	a/K =4.5	(8–16) POT	(8–16) 2BME	(6–16) 2BME	Expt.	a/K =4.5	(8–16) POT	(8–16) 2BME	(6–16) 2BME	Expt.
0.72	0.0	...	...	...	...	...	0.0038	0.012	0.012	0.013	0.0065±0.00013[a]
2.15	0.0	...	...	...	...	...	3.7	0.55	0.40	0.53	$0.49_{-0.07}^{+0.10}$
	0.72	3.82	4.09	4.91	1.64	0.05±0.018[b]	0.14	0.12	0.08	0.20	0.69±0.14[b]
	1.74	26.0	7.50	9.46	5.74	$1.51_{-0.21}^{+0.30}$	...	...	...	...	...
3.59	0.0	78.8	33.1	10.2	<0.3	$2.1_{-0.9}^{+1.7}$	11.0	14.2	17.6	18.9	$4.7_{-1.7}^{+1.0}$
	0.72	39.1	6.51	7.81	1.95	$0.35_{-0.35}^{+0.85}$[c]	12.1	19.6	28.3	27.0	$28.6_{-2.5}^{+3.1}$
	1.74	...	...	...	...	...	0.06	0.01	0.01	0.01	<0.15
	2.15	0.65	7.28	6.63	6.63	5.9± 0.7	0.28	0.32	0.21	0.22	0.86± 0.4
6.03	0.0	222	134	134	114	130 ±80[d]	942	1079	1074	1057	1300 ±400[d]

[a] Reference 19.
[b] These correspond to the larger magnitude of x ($E2/M1$). For the other possible value of x ($E2/M1$), the experimental values of $\Gamma_\gamma(M1)$ and $\Gamma_\gamma(E2)$ should be interchanged.
[c] This result is not significantly different from zero; to a confidence of 99.9% we can say that $\Gamma_\gamma(M1)<3.2\times10^{-4}$ eV.
[d] Reference 28.

Actually, Figs. 4–6 are given primarily to illustrate the approach, since all of the final information on the three mixing ratios comes from a simultaneous fit to all four of the angular distributions we have thus far considered. The results of this fit, partially displayed in Fig. 7, yield the following 0.1% limits for the $E2/M1$ mixing ratios of the three primary transitions: $3.59\rightarrow0$, $+0.21<x<+2.7$; $3.59\rightarrow0.72$, $-0.11<x^{-1}<+0.34$; $3.59\rightarrow2.15$, $-0.9<x<-0.22$. Note that the $M1/E2$ mixing ratio x^{-1} is given for the $3.59\rightarrow0.72$ transition rather than the $E2/M1$ mixing ratio. The best values of x to one standard deviation are listed in Table II. The best value for the mixing ratio of the $3.59\rightarrow0$ transition (Table II) was obtained by combining the present results with restrictions on $|x|$ from a previous study[23] of the angular correlation of the internal pairs associated with the $3.59\rightarrow0$ transition. The results for the other mixing ratios are consistent with the rather scanty information from previous work.[23,24] The alignment of the 3.59-MeV level corresponding to these best solutions is characterized by

$$P(0)=0.60\pm0.02,$$
$$P(1)=0.12\pm0.02,$$
$$P(2)=0.07\pm0.02.$$

IV. COMPARISON WITH THE IPM

A. $M1$ and $E2$ Radiative Widths

Experimental results pertaining to the γ decay of the B^{10} 2.15- and 3.59-MeV levels are collected in Table II. The $E2/M1$ mixing ratios are those of the present work, the branching ratios are those of Fig. 1, and the total radiative widths are those of Fisher *et al.*[25] All of the previous lifetime measurements[6,25–27] for the 2.15- and 3.59-MeV levels are in agreement; those of Fisher *et al.*[25] are adopted since they are close to the average of all measurements and are considerably more accurate than the previous results.[6,26,27]

Experimental results and also theoretical predictions for the $M1$ and $E2$ radiative widths are listed in Table III for the decay of the 2.15- and 3.59-MeV levels. Results for the 4^+, $T=0$, 6.03-MeV level[19,28] and the 1^+ 0.72-MeV level[19] are also included. The experimental values were extracted from the data of Table II and from Ref. 29 using the relations

$$\Gamma_\gamma(M1)=(1+x^2)^{-1}\Gamma_\gamma,\quad \Gamma_\gamma(E2)=[x^2/(1+x^2)]\Gamma_\gamma.$$

The IPM predictions for the radiative widths were calculated from the relations

$$\Gamma_\gamma(M1)=2.76\times10^{-3}E_\gamma{}^3\Lambda(M1)\text{ eV},$$
$$\Gamma_\gamma(E2)=8.02\times10^{-8}E_\gamma{}^5\Lambda(E2)\text{ eV},$$

where E_γ is in MeV and $\Lambda(M1)$ and $\Lambda(E2)$ are the transition strengths (as defined by Warburton and Pinkston[29]) obtained from the intermediate-coupling results of Kurath[4] for $a/K=4.5$ as well as from the various effective interaction results of Cohen and Kurath.[3] The (8–16) results are from a least-squares fit to data for nuclei in the range $A=8$–16, while the (6–16) results are from a fit to data in the range $A=6$–16. The three different effective interaction results [(8–16) POT, (8–16) 2BME, (6–16) 2BME] are defined and discussed by Cohen and Kurath.[3]

The $M1$ transition strengths $\Lambda(M1)$ are listed in Ref. 3. The $E2$ transition strength $\Lambda(E2)$ is proportional

[24] S. M. Shafroth and S. S. Hanna, Phys. Rev. **104**, 399 (1954).
[25] T. R. Fisher, S. S. Hanna, D. C. Healey, and P. Paul (to be published).
[26] J. A. Lonergan and D. J. Donahue, Phys. Rev. **139**, B1149 (1965); **145**, 998(E) (1965); D. J. Donahue, M. J. Wozniak, R. L. Hersberger, J. E. Cummings, and J. A. Lonergan, *ibid.* **165**, 1071 (1968).
[27] T. R. Fisher, S. S. Hanna, and P. Paul, Phys. Rev. Letters **16**, 850 (1966).
[28] D. E. Alburger, L. F. Chase, Jr., R. E. McDonald, and D. H. Wilkinson (to be published).
[29] E. K. Warburton and W. T. Pinkston, Phys. Rev. **118**, 733 (1960).

to the square of the radial integral $\rho=\langle r^2\rangle_{1p1p}$; in conformity with previous calculations in the $1p$ shell[7,29] we have taken ρ to be 7.056 F^2. The $E2$ transition strengths also include the effects of any collective enhancement. We have assumed that these effects can be simulated by endowing the neutron and proton with added charges $\beta_n e$ and $\beta_p e$ (the effective-charge approximation); for a self-conjugate nucleus the enhancement factor for $\Lambda(E2)$ is thus $\epsilon_{\Delta T}=[1+\beta_p+(-)^{\Delta T}\beta_n]^2$ for $\Delta T=0$ and 1 transitions.[7] We have taken $\beta_p=\beta_n=0.5$ so that $\epsilon_0=4.0$ and $\epsilon_1=1.0$. To obtain $\Gamma_\gamma(E2)$ for other values of ρ and $\epsilon_{\Delta T}$, say ρ' and $\epsilon_{\Delta T}'$, the values of Table III should be multiplied by $(\rho'/7.056)^2(\epsilon_{\Delta T}'/\epsilon_{\Delta T})$.[30] The assumed enhancement is admittedly rather arbitrary and, in fact, the variation of collective enhancement from transition to transition is a phenomenon that it would be desirable to elucidate by a comparison of this sort.

In Table IV we compare the experimental values of the $E2/M1$ mixing ratios (Table II) with the predictions[31] of the effective-interaction calculation of Cohen and Kurath.[3] The (8–16) 2BME predictions are shown and not the (6–16) 2BME predictions (see Table III), because although both results were generated from least-squares fits assuming the same effective interaction, the former seems more appropriate to mass 10. Similar comparisons for the $4^+\rightarrow 3^+$ $\Delta T=0$, $6.03\rightarrow 0$ transition[28] are also included. The two theoretical results are seen to be in fairly good agreement, but the predicted sign of $x(E2/M1)$ is in disagreement with experiment for three of the five transitions. Thus we conclude that a comparison of the radiative widths such as that of Table III (or of Ref. 6) is of limited value because for three of these five transitions the necessary condition that the sign of the mixing ratio be correctly predicted (Sec. I) has not been met.

Just how serious is the disagreement displayed in Table IV? That is, what is the overlap of a "correct" set of wave functions with those of Cohen and Kurath? One way to investigate this question is to perturb the wave functions slightly and then recalculate the $M1$ and $E2$ matrix elements, in order to examine the sensitivity of these matrix elements to the wave functions. We have done this via the following approximation. There are ten $J=1$, seven $J=2$, and ten $J=3$ states of p^6. We assume that the wave functions for the $J=1$ and $J=2$ B^{10} levels under consideration are given by a linear combination of the wave functions for the two that are lowest in energy:

$$\begin{aligned}\psi(0.72\text{-MeV level})&=\alpha(1)\psi(10)+\beta(1)\psi(10^*),\\ \psi(2.15\text{-MeV level})&=\beta(1)\psi(10)-\alpha(1)\psi(10^*),\\ \psi(3.59\text{-MeV level})&=\alpha(2)\psi(20)+\beta(2)\psi(20^*),\end{aligned}\quad(1)$$

where $\alpha(J)^2+\beta(J)^2=1$ and (JT) and (JT^*) designate the lowest and next-to-lowest energy levels of a given (JT). For simplicity we have mixed the $J=1$ and 2 states and not the $J=3$ states. There is some justification for this. The energy separation of the two lowest states of a given (JT) in the effective interaction calculation[3] is smallest for $(JT)=(10)$ with the next smallest separation being for $(JT)=(20)$. Thus, we expect the most trouble in separating the wave functions of the $J=1$ states, with the separation of the $J=2$ states next in difficulty. To illustrate, Cohen and Kurath found that the roles of the two lowest (10) states practically reversed between intermediate coupling (with $a/K=4.5$) and the (8–16) 2BME or (8–16) POT results. Furthermore, we see from Tables III and IV that the predictions for the $4^+\rightarrow 3^+$ $M1$ and $E2$ transitions are in excellent agreement with experiment so that we would not wish to perturb the $(JT)=(30)$ ground-state wave function unduly.[32]

We have chosen to perturb the (8–16) 2BME wave functions. The results would have been practically the same if we had used the (8–16) POT wave functions. The perturbed wave functions were generated by demanding an approximate accounting for the data on the $2.15\rightarrow 0.72$ and $3.59\rightarrow 0$ transitions. Excellent agreement with experiment was found for $\beta(1)=-\beta(2)=0.40$. (The agreement in magnitude of these two coefficients is accidental.) Theoretical results (labeled Pert.) for the five mixed $\Delta T=0$ transitions are compared to experiment in Table V. From this table we see that not only does this perturbation procedure bring the signs of *all* mixing ratios into agreement with experiment, but also the magnitudes of *both* the $M1$ and $E2$ radiative widths are considerably closer to experiment (compare the results of Tables III and V). For the three cases in which the sign of x $(E2/M1)$ has changed, the $M1$ matrix elements were responsible for the sign change; the $E2$ matrix elements are considerably less sensitive to changes in the wave functions.

With regard to these $E2$ matrix elements, we recall

TABLE IV. Quadrupole-dipole mixing ratios for transitions connecting the known $T=0$ s^4p^6 states of B^{10}.

$J_i^\pi\rightarrow J_f^\pi$	E_i (MeV)	E_f (MeV)	x $(E2/M1)$[a] (8–16) 2BME	(8–16) POT	Expt.
$1^+\rightarrow 1^+$	2.15	0.72	+0.13	+0.17	$-(3.75\pm0.55)^{\pm1}$
$2^+\rightarrow 3^+$	3.59	0.0	−1.25	−0.65	$+(1.5\ \pm0.6)$
$2^+\rightarrow 1^+$	3.59	0.72	-0.51^{-1}	-0.58^{-1}	$+(0.11\pm0.10)^{-1}$
$2^+\rightarrow 1^+$	3.59	2.15	−0.18	−0.21	$-(0.38\pm0.09)$
$4^+\rightarrow 3^+$	6.03	0.0	−2.82	−2.83	$-(3.16\pm0.12)$

[a] Calculated using $\epsilon_0=4.0$ and $\rho=7.056$ F^2. The phase convention is that of Ref. 7.

[30] To put the $\Lambda(E2)$ listed in Table II of Ref. 4 in our units they should be multiplied by $\rho^2\epsilon_{\Delta T}$, while the numerical values of $\Lambda(E2)$ given in Argonne National Laboratory Report No. ANL-7108 (Ref. 3) should be multiplied by $0.16\rho^2\epsilon_{\Delta T}$.

[31] D. Kurath (private communication).

[32] However, the $(40)\rightarrow(30)$ matrix elements are relatively insensitive to a perturbation like Eq. (1). We note that the sign of the $4\rightarrow 3$ mixing ratio is correctly given by the simple rotational model and the magnitudes of the $M1$ and $E2$ matrix elements are approximately reproduced by this model if we evaluate them in terms of the experimental electric-quadrupole and magnetic-dipole moments of the ground state.

TABLE V. Comparison of the predictions of the perturbed (8–16) 2BME results with experiment.

E_i (MeV)	E_f (MeV)	x $(E2/M1)$[a] Pert.	x $(E2/M1)$[a] Expt.	$\Gamma_\gamma(M1)$ (10^{-4} eV) Pert.	$\Gamma_\gamma(M1)$ (10^{-4} eV) Expt.	$\Gamma_\gamma(E2)$[a] (10^{-4} eV) Pert.	$\Gamma_\gamma(E2)$[a] (10^{-4} eV) Expt.
2.15	0.72	-2.73	$-(3.75\pm0.55)^{\pm1}$	0.046	0.05 ± 0.02[b]	0.34	0.69 ± 0.14[b]
	1.74	...	...	0.35	$1.51_{-0.21}{}^{+0.30}$	...	...
3.59	0.0	$+2.42$	$+1.5\ \pm0.6$	3.57	$2.1_{-0.9}{}^{+1.7}$	21.0	$4.7_{-1.7}{}^{+1.0}$
	0.72	$+0.22^{-1}$	$+(0.11\pm0.10)^{-1}$	1.15	$0.35_{-0.35}{}^{+0.85}$	23.1	$28.6_{-2.5}{}^{+3.1}$
	2.15	-0.30	$-(0.38\pm0.09)$	5.16	$5.9\ \pm0.7$	0.46	0.86 ± 0.4

[a] Calculated using $\epsilon_0=4.0$ and $\rho=7.056$ F^2. The phase convention is that of Ref. 7.
[b] These correspond to the larger magnitude of x $(E2/M1)$. For the other possible value of x $(E2/M1)$ the experimental values of $\Gamma_\gamma(M1)$ and $\Gamma_\gamma(E2)$ should be interchanged.

TABLE VI. Radiative widths and $E2/M1$ mixing ratios for the decay of the $J^\pi=2^+$, $T=1$ 5.16-MeV level of B^{10}.

E_f (MeV)	Branching ratios[a] (%)	$\Gamma_\gamma(M1)$ (eV) Expt.[a]	$\Gamma_\gamma(M1)$ (eV) (8–16) 2BME[c]	$\Gamma_\gamma(M1)$ (eV) Pert.[d]	x $(E2/M1)$[b] Expt.[e]	x $(E2/M1)$[b] (8–16) 2BME[c]	x $(E2/M1)$[b] Pert.[d]
0	5.1 ± 0.7	0.14 ± 0.06	0.45	0.45	$+(0.17_{-0.13}{}^{+0.30})$	$+0.023$	$+0.023$
0.72	27.6 ± 2	0.76 ± 0.30	0.013	0.27	$\lvert x\rvert\leqslant0.1$	-0.015	-0.016
2.15	61.0 ± 2	1.68 ± 0.66	0.75	0.67	$\lvert x\rvert\leqslant0.1$	-0.011	-0.011
3.59	6.3 ± 1	0.17 ± 0.08	0.12	0.17	f	$+0.003$	$+0.003$

[a] These were obtained by combining the results of Refs. 5, 33, and 34.
[b] Calculated assuming $\epsilon_1=1.0$ and $\rho=7.056$ F^2. The phase convention is that of Ref. 7.
[c] From Ref. 3.
[d] Obtained from a perturbation of the results of Ref. 3 as explained in the text.
[e] L. Meyer-Schützmeister and S. S. Hanna, Phys. Rev. **108**, 1506 (1957).
[f] Assumed to have negligible $E2$ contribution.

that an effective charge of 0.5 electronic units was used in calculating $\Lambda(E2)$ for $\Delta T=0$ transitions. In as far as the rotational model is applicable to B^{10}, the transitions considered here are all interband transitions and thus, in this model, the collective enhancement—parametrized by the effective charge—is sensitively dependent on the amount of band mixing. We should expect variation of the effective charge between 0 and ~0.5 electronic units resulting in overestimation of $\Gamma_\gamma(E2)$ by up to a factor of 4 for $\Delta T=0$ transitions. This should be kept in mind in our comparisons of theory and experiment.

To further test the perturbed wave functions we compare, in Table VI, the predicted $M1$ radiative widths for the decay of the lowest $(JT)=(21)$ state with the experimental results for the 5.16-MeV level with which it is identified.[5,33,34] It is seen that the perturbation largely removes the one serious disagreement with experiment—that involving the $M1$ width of the $5.16\rightarrow0.72$ transition.

Our perturbation procedure appears to be quite successful. We note that experiment allowed two values for the mixing ratio of the $2.15\rightarrow0.72$ transition and it is only possible to reproduce the one with the larger magnitude by our procedure. Thus, a determination of this mixing ratio would provide one test of the perturbed wave functions.

What is the significance of the success of this perturbation procedure? At the least we can say that it illustrates the extreme sensitivity of the matrix elements to changes in the wave functions since only 16% (in intensity) of the "other" wave functions need be admixed for both $J=1$ and 2. Thus we may conclude that the wave functions of Cohen and Kurath are probably quite close to the truth. We have not answered the question as to whether or not it is possible to find an effective interaction that would give rise to the perturbed wave functions, or ones approximating them. Intuitively, we feel it is likely that an acceptable interaction could be found that would fit these radiative widths and mixing ratios satisfactorily, that would not cause significant alteration of the parameters of the effective interaction,[3] and that would not significantly change the predicted energy-level scheme of this and neighboring nuclei.[35] The search for such an interaction may be quite difficult but is obviously of much interest.

ACKNOWLEDGMENTS

We are indebted to Dieter Kurath for counsel, caution, and calculations, and to T. R. Fisher, P. Paul, and S. S. Hanna for communications concerning their measurements of the lifetimes of the 2.15- and 3.59-MeV levels.

[33] E. K. Warburton, D. E. Alburger, and D. H. Wilkinson, Phys. Rev. **132**, 776 (1963).
[34] R. E. Segel and R. H. Siemssen, Phys. Letters **20**, 295 (1966); P. Paul, T. R. Fisher, and S. S. Hanna, *ibid.* **24B**, 51 (1967).
[35] This point is disscused in Sec. 4.10 of Ref. 3.